



**HAL**  
open science

## Determination of the dried product resistance variability and its influence on the product temperature in pharmaceutical freeze-drying

Bernadette Scutella, Ioan-Cristian Trelea, Erwan Boulrés, Fernanda Fonseca, Stéphanie Passot

### ► To cite this version:

Bernadette Scutella, Ioan-Cristian Trelea, Erwan Boulrés, Fernanda Fonseca, Stéphanie Passot. Determination of the dried product resistance variability and its influence on the product temperature in pharmaceutical freeze-drying. *European Journal of Pharmaceutics and Biopharmaceutics*, 2018, 128, pp.379-388. 10.1016/j.ejpb.2018.05.004 . hal-01789065

**HAL Id: hal-01789065**

**<https://agroparistech.hal.science/hal-01789065>**

Submitted on 9 May 2018

**HAL** is a multi-disciplinary open access archive for the deposit and dissemination of scientific research documents, whether they are published or not. The documents may come from teaching and research institutions in France or abroad, or from public or private research centers.

L'archive ouverte pluridisciplinaire **HAL**, est destinée au dépôt et à la diffusion de documents scientifiques de niveau recherche, publiés ou non, émanant des établissements d'enseignement et de recherche français ou étrangers, des laboratoires publics ou privés.

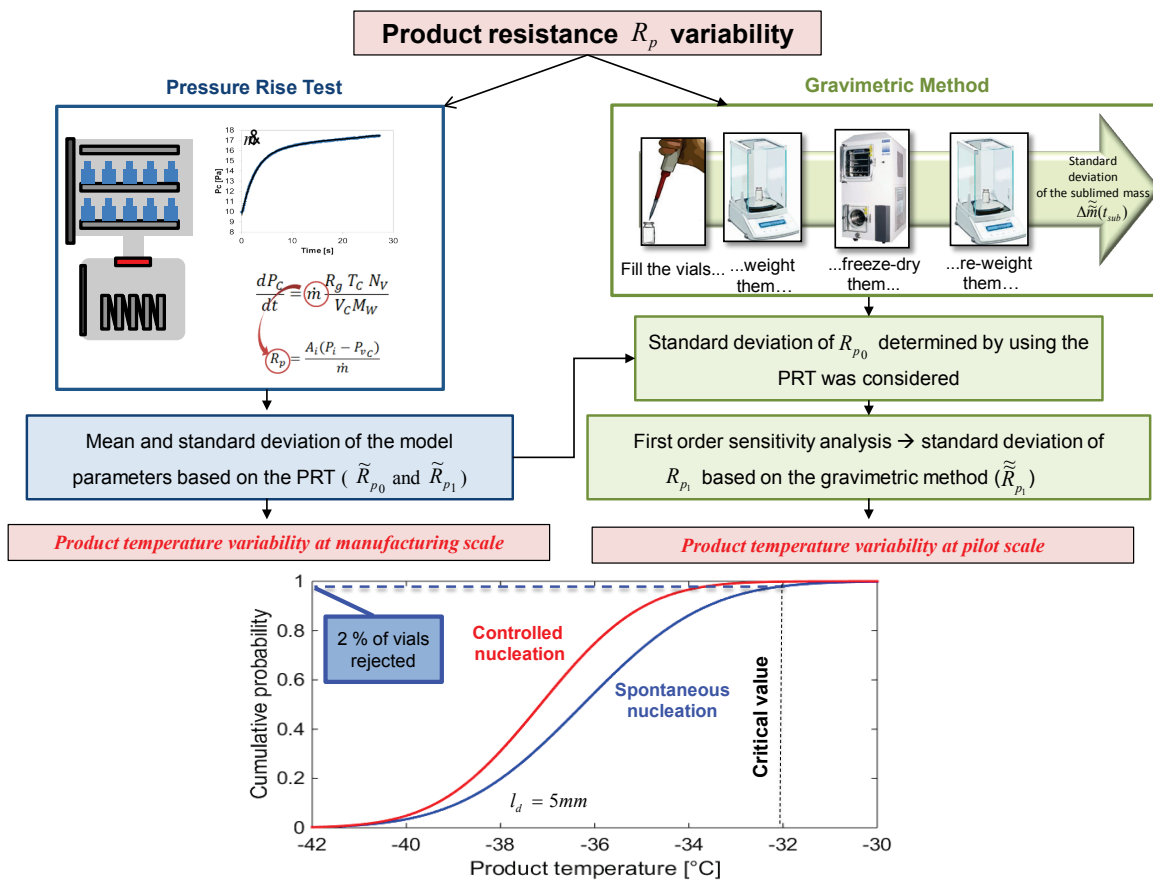
# Determination of the dried product resistance variability and its influence on the product temperature in pharmaceutical freeze-drying

Authors: Bernadette Scutellà<sup>1,2</sup>, Ioan Cristian Trelea<sup>2</sup>, Erwan Bourlès<sup>1</sup>, Fernanda Fonseca<sup>2</sup>,  
Stephanie Passot<sup>2</sup>

<sup>1</sup> GSK Biologicals SA, Rixensart, Belgium

<sup>2</sup> UMR GMPA, AgroParisTech, INRA, Université Paris Saclay, 78850 Thiverval-Grignon,  
France

## Graphical abstract



## **Abstract**

During the primary drying step of the freeze-drying process, mass transfer resistance strongly affects the product temperature, and consequently the final product quality. The main objective of this study was to evaluate the variability of the mass transfer resistance resulting from the dried product layer ( $R_p$ ) in a manufacturing batch of vials, and its potential effect on the product temperature, from data obtained in a pilot scale freeze-dryer. Sublimation experiments were run at  $-25\text{ }^\circ\text{C}$  and 10 Pa using two different freezing protocols: with spontaneous or controlled ice nucleation. Five repetitions of each condition were performed. Pressure rise test (PRT) and gravimetric methods were applied as complementary approaches to estimate  $R_p$ . The PRT allowed to assess variability of the evolution of  $R_p$  with the dried layer thickness between different experiments whereas the gravimetric method informed about  $R_p$  variability at a fixed time within the vial batch. A product temperature variability of approximately  $\pm 4.4\text{ }^\circ\text{C}$  was defined for a product dried layer thickness of 5 mm. The present approach can be used to estimate the risk of failure of the process due to mass transfer variability when designing freeze-drying cycle.

**Keywords:** lyophilisation, drying, mass transfer, product resistance, sublimation rate, controlled nucleation, heterogeneity, distribution, pressure rise test

## 1. Introduction

Freeze-drying is a gentle-drying process which consists of the dehydration of the frozen product under-vacuum by sublimation followed by desorption. This process is currently the method of choice in the pharmaceutical industry for the preservation of heat sensitive products (such as vaccines, proteins or micro-organisms) [1-3]. Several quality attributes of these products, e.g. the visual aspect of the dried cake, the reconstitution time and the moisture content, are governed by the product temperature profile during the sublimation step [4-6]. If the temperature of the sublimation interface exceeds a critical value, i.e. collapse temperature, the product may experience abrupt loss of quality resulting from the collapse of its dried porous structure [4-6].

The thermal history of the product cannot be directly controlled but it is determined by the heat and mass transfer occurring during the process. Mathematical models derived from theoretical considerations of these phenomena are extensively used to predict the product temperature, for process design and scale-up [7-13]. Freeze-drying models involve the determination of heat and mass transfer parameters, such as the vial heat transfer coefficient  $K_V$  and the mass transfer resistance due to the dried layer of the product  $R_p$  [7, 10, 12, 13]. The accurate evaluation of these model parameters and their variability is of paramount importance for a reliable prediction of the product temperature within the vials batch and between different freeze-dryers.

The vial heat transfer coefficient  $K_V$  is specific for the container, and depends on the chamber pressure and on the dimensions of the vial bottom geometry. It is usually determined by the gravimetric method [12, 14-16], which allows to have a detailed picture of the variability of this parameter among the vials on the shelf. In contrast, the product resistance  $R_p$  highly depends on the formulation and on the freezing protocol. Its value continuously increases with the increase of the dried layer thickness.

In literature, several methods were proposed to measure the evolution of the product resistance along with the changes in the dried layer thickness by estimating the mass flow rate value, such as the microbalance [17, 18], the Pressure Rise Test (PRT) [19-21], the Tunable Diode Laser Absorption Spectroscopy (TDLAS) [22]. Product resistance can also be estimated from the product temperature profile recorded by thermal sensors during the process by using mathematical models and soft sensors (or software sensors) [23, 24]. Some of these techniques, such as the PRT and the TDLAS, provide a global value of the product resistance in the vial batch, from the measurement of the global mass flow rate. Other

methods allow to determine product resistance evolution in one vial (such as the microbalance) or in a limited number of vials (for example the use of thermocouples). Thus, the determination of the variability of the product resistance within a manufacturing batch of vials remains particularly challenging.

The product resistance value and variability are directly influenced by the freezing step. Some authors have shown a direct correlation between nucleation temperature, ice crystal size, and mass transfer during sublimation [20, 25, 26]. It was reported that high values of nucleation temperature generate few and large ice crystals, which upon sublimation leave larger pores and smaller specific surface area than low values of nucleation temperature. The dimension of the pores dramatically influences the resistance of the product due to the dried layer, and thus the sublimation rate [25, 27]. Furthermore, the stochastic nature of nucleation temperature leads to different kinetics of sublimation within a same vial batch [20, 28, 29], resulting in potentially high vial to vial variability that would make it difficult to achieve homogeneous product quality.

In the present work, the product resistance  $R_p$  in a manufacturing batch of vials was estimated from data obtained at pilot scale. Sublimation experiments were performed using a 5 % sucrose solution at 10 Pa and -25 °C in a pilot scale freeze-dryer. Two different freezing protocols were used, i.e. the nucleation of ice crystals was either spontaneous or controlled using a nucleating agent. Five repetitions of each condition were carried out, in order to evaluate the product resistance variability between different pilot scale batches. Two additional cycles with partially stoppered vials were carried out, to study the effect of the presence of the stopper on the mass transfer resistance. Two experimental methods were used for the determination of the product resistance: (1) a global/batch one, namely the pressure rise test (PRT), to evaluate the average evolution of the product resistance with the dried layer thickness in single batches, and (2) a local/single vial one, namely the gravimetric method, to evaluate the variability of the mass loss between single vials at a given dried layer thickness. The use of the global/batch method can provide an estimation of the product resistance variability in a large batch of vials (manufacturing scale), from repetitions of cycles performed at pilot scale, whereas the use of the local/single vial method can provide a estimation of the product resistance variability within a small batch (pilot scale). Finally, the effect of  $R_p$  variability on the product quality was quantified by calculating the product temperature distribution and by assessing the risk of failure (potential percentage of collapsed vials) during the sublimation step.

## **2. Materials and Methods**

### **2.1. Materials**

Siliconized 3 mL tubing vials (Müller + Müller, Holzminden, Germany) filled with a 5 % w/w aqueous sucrose solution were used throughout this study.

The experiments were carried out using a pilot scale freeze-dryer (REVO model, Millrock Technology, Kingston, NY, United States). This device included three temperature controlled shelves and a condenser connected to the drying chamber by a butterfly valve. The drying chamber had a volume of 0.12 m<sup>3</sup>. Two pressure gauges, a capacitance manometer (MKS) and a thermal conductivity gauge (Pirani) were used to monitor the pressure in the chamber. In order to monitor the product temperature during the cycles, 7 type-T thermocouples were placed in the bottom center of selected vials (Fig. 1).

### **2.2. Freeze-drying cycles**

A total of 204 vials were arranged in hexagonal clusters (Fig. 1) on a bottomless tray and filled with 1.8 mL of the sucrose solution (i.e., ~ 10 mm of filling height and ~ 10.9 mm after freezing). In order to minimize the additional heat transfer at the border of the shelf, the vial batch was fully shielded by a polystyrene rail covered by aluminum tape. The use of this rail allowed to decrease the heat transfer ratio between edge and central vials to 150% from an initial value of 200 % determined in case of vials completely exposed to the walls of the drying chamber. Three experimental conditions were investigated, as presented in Table 1: vials filled with 5 % sucrose solution and processed without stoppers and with spontaneous nucleation (S5); vials filled with sucrose solution and processed with partially inserted stoppers and with spontaneous nucleation (S5s); vials filled with sucrose and nucleating agent Snomax solution and processed without stopper and with controlled nucleation (S5cn). The sucrose solution was not filtered before use, and no specific vial washing procedure was applied. The filling operation and the freeze-dryer loading were not carried out in a clean environment.

Sublimation experiments with spontaneous nucleation (referred as S5) were performed as follow: (1) a freezing step, performed firstly by cooling the shelf at 3 °C min<sup>-1</sup> from ambient temperature to -50 °C and then by holding the vials for 2 h at -50 °C, and (2) a sublimation step, carried out at a shelf temperature of -25 °C (heating rate of approximately 2.5 °C min<sup>-1</sup>) and a chamber pressure of 10 Pa. When controlled nucleation was applied, 0.1 % (w/w) of the nucleation agent Snomax (Snomax LLC, Englewood, CO, US), an active protein derived

from *Pseudomonas syringae*, was added to the sucrose solution and the following freezing protocol was applied. The shelf temperature was at first decreased from ambient temperature to -4 °C at approximately 3 °C min<sup>-1</sup>, then maintained at -4 °C for 1 hour to initiate ice nucleation and finally decreased to -50 °C at 3 °C min<sup>-1</sup>. The occurrence of ice nucleation was verified by visual inspection through the plexiglass door and by thermocouple data monitoring. A summary of all the performed experiments is presented in Table 1.

The pressure rise tests (PRT) were performed to determine the mass flow rate for all the experimental conditions (S5, S5s and S5cn). The PRT consisted in closing the valve between the drying chamber and the condenser at specified moments for a short time period of 30s. The manometric pressure was recorded during the PRT every 0.1 s by an in-house software. Some cycles (two of each condition without stopper) were stopped at approximately 30 % of the total sublimation time (approximately 16 h) and the sublimed ice mass in 50 central vials (marked with the letter M in Fig. 1) was determined by the gravimetric method, as proposed by Scutella et al. [16]. The selected vials were weighed before and after the cycle, and the water loss was calculated as difference between initial and final vial mass. For each freezing condition, a total of 100 vials were studied. The standard deviation of the sublimed ice mass  $\Delta\overline{m}(t_{sub})$  of the considered vial batch was then calculated from the water loss data.

### 3. Theory and data analysis

#### 3.1. Theoretical description of the product resistance

##### 3.1.1. Evaluation of the product resistance from the mass flow rate

As widely reported in literature [12, 24, 30-33], the product resistance  $R_p$  can be calculated as:

$$R_p = \frac{A_i(P_i - P_{vC})}{\dot{m}} \quad (1)$$

where  $\dot{m}$  is the mass flow rate,  $A_i$  is the inner bottom area of the vials,  $P_{vC}$  is the partial pressure of the vapour in the drying chamber, usually assumed to be equal to the total chamber pressure during the sublimation step, and  $P_i$  is the vapour pressure at the sublimation interface, calculated using the Clausius-Clapeyron relation [16]:

$$P_i = e^{-\frac{6139.6}{T_i} + 28.8912} \quad (2)$$

In Eq. (2),  $T_i$  is the product temperature at the sublimation interface theoretically determined from the heat balance at the vial scale. The heat flow through the frozen product layer was expressed as:

$$\dot{Q} = A_i \frac{\lambda_f}{l_f} (T_i - T_{BV}) \quad (3)$$

where  $T_{BV}$  is the product temperature at the vial bottom,  $\lambda_f$  is the conductivity of the frozen layer,  $A_i$  is the sublimation interface area, considered equal to the internal cross sectional area of the vial,  $l_f$  is the frozen layer thickness, evaluated as the difference between the initial product thickness and the dried layer thickness at a specific time and  $\dot{Q}$  is the heat flow rate, which is equal to the latent heat of sublimation  $\Delta H$  times the mass flow rate  $\dot{m}$  under steady state conditions:

$$\dot{Q} = \Delta H \dot{m} \quad (4)$$

The product temperature  $T_{BV}$  is calculated based on the heat flow rate between the shelf and the vial bottom [12, 16]:

$$\dot{Q} = A_{BV} K_V (T_{BV} - T_S) \quad (5)$$

where  $A_{BV}$  is the outer vial bottom area, considered equal to external cross sectional area of the vial,  $T_S$  is the temperature of the shelf, evaluated as the average between the inlet and outlet shelf fluid temperatures, and  $K_V$  is the vial heat transfer coefficient evaluated as proposed by Scutellà et al. [16].

All relevant physical product properties and parameters used are reported in Table 2.

### 3.1.2. Dependence of the product resistance on the dried layer thickness $l_d$

The product resistance  $R_p$  can be described as a linear function of the dried layer  $l_d$  [6, 12]:

$$R_p = R_{p_0} + R_{p_1} l_d \quad (6)$$

where  $R_{p_0}$  and  $R_{p_1}$  are coefficients determined by data regression. The evolution of dried layer thickness in time ( $\frac{dl_d}{dt}$ ) can be calculated as:

$$\frac{dl_d}{dt} = \frac{1}{\rho A_i} \dot{m} \quad (7)$$

where  $\rho$  is the density of the ice.

### 3.2. Experimental evaluation of $R_p$ and calculation of $R_p$ distribution

The value of product resistance  $R_p$  continuously evolves during sublimation with the increase of the dried layer thickness (Eq. 6). However, the evolution of  $R_p$  with  $l_d$  may vary from one vial to the other within the same batch.

Fig. 2 schematically represents the strategies used to evaluate the variability of the product resistance values at given  $l_d$  for specific experimental conditions, between batches and within the same batch. Two experimental methods were used: a batch/global method (pressure rise test) and a single vial/local method (gravimetric method). The combination of data from several pilot scale vial batches was assumed to make it possible to simulate a large vial batch similar to those observed at manufacturing scale. To our knowledge, no methods were published before to estimate the variability of  $R_p$  in a large batch of vials.

#### 3.2.1. Evaluation of $R_p$ using the batch method (pressure rise test)

Pressure rise tests (PRT) were used to determine the average mass flow rate among 204 vials during the sublimation step for all performed experiments. Fig. 3 shows an example of the evolution of the chamber pressure during a PRT. As soon as the valve between the chamber and the condenser was closed, the pressure inside the chamber increased, due to the accumulation of the sublimed ice mass. The pressure initially increased very rapidly and it raised slower when the chamber pressure approached the equilibrium value with the ice surface [19].

The initial slope of the pressure rise curve  $\frac{dP_C}{dt}$  was calculated by fitting the data with a 6<sup>th</sup> degree polynomial equation and by performing the analytical first derivative at the initial pressure rise time. Then,  $\frac{dP_C}{dt}$  was considered directly proportional to the sublimation mass flow rate  $\dot{m}$  through the ideal gas law:

$$\frac{dP_C}{dt} = \dot{m} \frac{R_g T_C N_V}{V_C M_W} \quad (8)$$

where  $R_g$  is the ideal gas constant,  $V_C$  is the volume of the drying chamber,  $T_C$  is the temperature of the chamber, estimated as an average between the shelf temperature and product temperature at the interface [15],  $M_W$  is the molecular weight of the water vapour and  $N_V$  is the number of vials. The values of the relevant physical properties used in Eq. (8) are reported in Table 2.

The mass flow rate values obtained from the PRT were then used to calculate the product resistance evolution along with the dried layer thickness increase by using Eqs. (1)-(5), as reported in §3.1.1. For each tested freezing condition (i.e. S5 and S5cn), five curves were obtained. The curves were considered as a single set of data to fit Eq. (6) and to calculate the values and the standard errors ( $SE$ ) of the parameters  $R_{p_0}$  and  $R_{p_1}$ . Finally, the standard deviations ( $SD$ ) of the product resistance parameters  $R_{p_0}$  and  $R_{p_1}$  (named  $\widetilde{R}_{p_0}$  and  $\widetilde{R}_{p_1}$ ), were calculated from the  $SE$  by considering:

$$SD = SE\sqrt{df} \quad (9)$$

where  $df$  is the number of the degrees of freedom (equal to approximately 100 in the present study), equal to the difference between the number of experimental points collected (i.e. the total number of PRTs performed during the five experiments for each condition) and the number of parameters ( $R_{p_0}$  and  $R_{p_1}$  for Eq. (6)). Calculations were performed with MATLAB R2014b software (The MathWorks, Inc., Natick, MA).

### 3.2.2. Evaluation of $R_p$ using a single vial method (gravimetric method)

The variability of the product resistance was evaluated in terms of the standard deviation  $\widetilde{R}_{p_1}$  which was estimated for a small pilot batch of 100 vials by performing a variance-based sensitivity analysis [34] (Fig. 2, right hand side). The gravimetric method was used to determine the standard deviation of the sublimated ice mass at a given time  $\widetilde{\Delta m}(t_{sub})$  among vials in freeze-drying cycles carried out with spontaneous (S5-4 and S5-5, Table 1) and controlled (S5cn-4 and S5cn-5, Table 1) nucleation. Differences in the sublimated ice mass between vials can be due to the variability of the heat transfer to the vial and of the mass transfer in the dried layer. Thus, the total variance of the sublimated mass  $\widetilde{\Delta m}(t_{sub})^2$  can be

expressed as the sum of the fractions of variances stemming from the heat and mass transfer parameters  $K_V$ ,  $R_{p_0}$  and  $R_{p_1}$ , assuming that their effects are independent:

$$\Delta m(\widetilde{t_{sub}})^2 = \left(\frac{\partial \Delta m(t_{sub})}{\partial K_V}\right)^2 \widetilde{K_V}^2 + \left(\frac{\partial \Delta m(t_{sub})}{\partial R_{p_0}}\right)^2 \widetilde{R_{p_0}}^2 + \left(\frac{\partial \Delta m(t_{sub})}{\partial R_{p_1}}\right)^2 \widetilde{R_{p_1}}^2 \quad (10)$$

where  $\frac{\partial \Delta m(t_{sub})}{\partial K_V}$ ,  $\frac{\partial \Delta m(t_{sub})}{\partial R_{p_0}}$  and  $\frac{\partial \Delta m(t_{sub})}{\partial R_{p_1}}$  represent the sensitivities of  $\Delta m(t_{sub})$  to the parameters  $K_V$ ,  $R_{p_0}$  and  $R_{p_1}$  respectively. These sensitivities were estimated using a finite difference method [35]:

$$\frac{\partial \Delta m(t_{sub})}{\partial \varphi_i} = \frac{\Delta m(t_{sub})(\varphi_i + \delta) - \Delta m(t_{sub})(\varphi_i)}{\delta} \quad (11)$$

where  $\varphi_i$  represents each considered parameter ( $K_V$ ,  $R_{p_0}$  or  $R_{p_1}$ ) and  $\delta$  an increment equal to 5 % of  $\varphi_i$ . Eq. (11) was solved as follow. Firstly, Eq. (1)-(6) were used to calculate the mass flow rate  $\dot{m}$  by considering the mean value of  $R_{p_0}$  and  $R_{p_1}$  previously determined with the PRT method, and the  $K_V$  value measured as proposed by Scutellà et al. [16]. Then, the term  $\Delta m(t_{sub})$  was calculated by integrating the mass flow rate over time  $t_{sub}$  (sublimation time). The sublimation time was measured from the moment when shelf temperature exceeded product temperature, meaning that there was a net heat flux from the shelf towards the vials. The calculation was repeated considering the  $i$ -parameter incremented by  $\delta$ .

The sensitivity terms obtained for each of the considered parameters were used in Eq. (10) to calculate the standard deviation of  $R_{p_1}$  based on the gravimetric method (namely  $\widetilde{R_{p_1}}$ ). As only central vials were analyzed, the standard deviation of  $K_V$  ( $\widetilde{K_V}$ ) was considered as mainly due to the vial bottom geometry and determined as proposed by Scutellà et al. [16] (Table 2). The standard deviation of  $R_{p_0}$  was taken to be approximately equal to  $\widetilde{R_{p_0}}$ , previously determined using the PRT method.

Finally, the normally distributed random values of  $R_{p_0}$  and  $R_{p_1}$  were used in Eq. (6) to calculate the product resistance distribution for a specific  $l_d$ . The software MATLAB R2014b equipped with the Statistics Toolbox (The MathWorks, Inc., Natick, MA) was used to perform the calculations.

### 3.3. Evaluation of the product temperature $T_{BV}$ distributions

In order to assess the impact of the product resistance variability on the final product quality, distributions of the product temperature  $T_{BV}$  were calculated at a specific  $l_d$  from the previously determined  $R_p$  distributions using Eq. (1)-(5). For this calculation,  $K_V$  was set equal to its mean value. Chi-square goodness-of-fit tests were performed on the product temperature distributions, to verify that the simulated data were compatible with a normal distribution at a 0.05 significance level.

## 4. Results and Discussion

### 4.1. Effect of the stopper and of the freezing protocol on the mass flow rate

Fig. 4 shows the mass flow rates evolution with dried layer thickness  $l_d$  determined by PRT for batches of vials processed with and without stoppers and frozen by following two different protocols: spontaneous and controlled nucleation. The mass flow rate decreased as the dried layer thickness increased regardless of the experimental condition. However, at a dried layer thickness of approximately 7 mm, the mass flow rate started to decrease significantly. This type of behaviour of PRT data was previously reported in literature and was ascribed to batch heterogeneity [19]. A constant number of sublimating vials was continuously considered in the data analysis ( $N_V$  in Eq. (8)), whereas the vials in the batch completed sublimation at different times. Furthermore, it was assumed that the ice-vapour interface area ( $A_i$ , Eqs. (1), (3) and (7)) was flat and it remained constant during sublimation. However, previous works [36, 37] showed that the shape of  $A_i$  may change during sublimation and can vary for vials located at different positions on the shelf. The uncertainty of the PRT at the end of sublimation impacts on the determination of the mass flow rate and thus on the determination of the dried layer thickness (which can be observed to vary in Fig. 4 between 10 mm and 11.2 mm, compared to an initial frozen layer of 10.9 mm).

The absolute value of the slope of the Pirani gauge signal observed at the end of sublimation can be used as an indication of the heterogeneity of the sublimation rates in the batch, as previously proposed in literature by Passot et al. [28]. Fig. 5 presents the absolute values of the Pirani slope for cycles performed with and without stoppers and with and without controlled nucleation. The results shows that the presence of the stoppers on the vials (S5s) had no significant impact on the value of the Pirani slope and thus on the heterogeneity of the sublimation rates (at a 0.05 significance level). However, the addition of the nucleation agent

Snomax (*Pseudomonas syringae*) which allows to control ice nucleation (S5cn), significantly increases the value of the Pirani slope and thus the homogeneity in the vial batch.

Fig. 6 shows the average values of the sublimation mass flow rate (between dried layer thickness of 0.5 mm and 7 mm; total dried layer is of 10.9 mm) for each freeze-drying cycle performed with and without partially inserted stoppers and with and without controlled nucleation during the freezing step. ANOVA test at 0.05 significance level revealed that the presence of the stoppers on the vials did not add a significant resistance to the mass transfer from the ice-vapour interface to the chamber. This finding is in agreement with an earlier work of Pikal et al. [12], who quantified the relative importance of the stopper resistance to be approximately 3-10 % of the total mass transfer resistance, which is negligible compared to the product resistance (80-90 %). Conversely, the use of controlled nucleation by adding the nucleation agent Snomax to the solution (S5cn) significantly increased the mass flow rate as compared to spontaneous nucleation (S5) of 11 %, as already reported in literature [25, 28]. However, in the present work the increase of mass flow rate resulting from the use of controlled nucleation is relatively low compared to the results reported by Searles et al. [25], who reported an increase of the mass flow rate of 60 % between vials processed with and without *Pseudomonas syringae*. This result could be ascribed to two experimental observations: (i) the high value of cooling rate applied (3 °C/min) could have limited the ice crystal growth after nucleation [38] and (ii) the high value of nucleation temperature observed when spontaneous nucleation was applied ( $-4.39 \pm 2.02$  °C). Searles et al. [25] reported a value of -11.4 °C for spontaneous nucleation. This higher value could be explained by a higher level of particles in the sucrose solution due to the non application of specific procedures for washing, filling the vials and loading the freeze-drying (i.e., non filtration of the solution and non control of the level of particles in the environment).

#### **4.2. Determination of the product resistance variability**

The evaluation of the mass transfer variability within a manufacturing batch (often constituted by more than 100,000 vials) represents a real challenge. In the present work, the inter-vial mass transfer variability within a manufacturing batch was estimated by combining product resistance data from replicates of small batches processed in a pilot scale freeze-dryer with and without controlled nucleation (5 batches for each freezing condition). The evolution of the product resistance  $R_p$  with the dried layer thickness was calculated from the mass flow rate values obtained using the PRT in cycles performed with and without controlled

nucleation (S5 and S5cn). Fig. 7 shows that the product resistance increased linearly with the dried layer thickness, regardless of the applied freezing protocol. Eq. (6) was then used to fit the product resistance data obtained from cycles S5 and S5cn performed with spontaneous nucleation (Fig. 7A) and controlled nucleation (Fig. 7B), respectively. The obtained values and standard deviations of the two sets of parameters  $R_{p_0}$  and  $R_{p_1}$  are reported in Table 3. Both the parameters  $R_{p_0}$  and  $R_{p_1}$  exhibited greater values and also greater standard deviations for cycles performed with spontaneous nucleation (data set S5) than for cycles performed with controlled nucleation (data set S5cn). The value of  $R_{p_0}$  (59 and 47  $kPa\ m^2\ s/kg$  for S5 and S5cn data sets, respectively) appeared to be of the same order of magnitude as previously reported values for sucrose-based model formulation (e.g. 51.2  $kPa\ m^2\ s/kg$  [39] and 10  $kPa\ m^2\ s/kg$  [13]), whereas  $R_{p_1}$  appeared to be lower ( $<1.8\ 10^4\ kPa\ m^2\ s/kg$ ) than the value determined by Pisano et al. [13] ( $1.65\ 10^5\ kPa\ m^2\ s/kg$ ). The determined coefficients  $R_{p_0}$  and  $R_{p_1}$  were used in Eq. (6) to calculate the value of the product resistance at a dried layer thickness of 5 mm, which was compared in Table 4 with relevant data reported in literature [24, 26, 32, 40]. Regardless of the freezing protocol, the values of  $R_p$  determined in this study appeared to be in good agreement with the previously published values, and in particular with the  $R_p$  value evaluated by Bosca et al. [24] under spontaneous nucleation and by Konstantinidis et al. [26] under controlled nucleation.

The gravimetric method was then used to evaluate the inter-vial product resistance variability of pilot scale batches at a given dried layer thickness. The distribution and standard deviation of the sublimed ice mass at a specific time ( $\Delta\tilde{m}(t_{sub})$ ) were determined in a batch of 100 vials processed with and without controlled nucleation and are reported in Fig. 8. The value of  $\Delta\tilde{m}(t_{sub})$  appeared to be lower for product processed with controlled nucleation than with spontaneous nucleation. The standard deviation values  $\Delta\tilde{m}(t_{sub})$  were used in Eq. (10) to calculate the value of standard deviation of  $R_{p_1}$  based on the gravimetric method (namely  $\tilde{R}_{p_1}$ ) for cycles S5 and S5cn, which is reported in Table 3. The standard deviation  $\tilde{R}_{p_1}$  based on the gravimetric method represents approximately 15-20 % of the corresponding mean value of  $R_{p_1}$ , which is comparable to the 10-25 % reported in the literature [13, 39]. However, this standard deviation  $\tilde{R}_{p_1}$ , which is representative for the variability of a pilot scale batch, was found to be about 5 to 6 times lower than the standard deviation  $\tilde{R}_{p_1}$  obtained from the PRT, which is assumed to be representative for manufacturing batches and especially of the stochastic nature of spontaneous nucleation. For the following analysis of

product temperature distribution, this greater variability based on  $\widetilde{R}_{p_0}$  and  $\widetilde{R}_{p_1}$  was used since it could better reflect the product heterogeneity at manufacturing scale.

Finally, the value and standard deviation of the model parameters  $R_{p_0}$  and  $R_{p_1}$  determined by PRT for cycles carried out with and without controlled nucleation was used to evaluate the distribution of the product resistance. The obtained cumulative probability curves of  $R_p$  are shown in Fig. 9 for a chamber pressure of 10 Pa and a shelf temperature of -25 °C. Products processed with spontaneous (Fig. 9A) and controlled nucleation (Fig. 9B) during the freezing step were considered. The simulation was carried out for two values of dried layer thickness, 1 mm and 5 mm (total product thickness equal to 10 mm).

The results show that the standard deviation of the product resistance significantly increased with  $l_d$ . In particular, product resistance values can be defined in a range of approximately  $\pm 160 \text{ kPa s m}^2 \text{ kg}^{-1}$  at 1 mm and of approximately  $\pm 280 \text{ kPa s m}^2 \text{ kg}^{-1}$  at 5mm for product processed with spontaneous nucleation (Fig. 9A), and from  $\pm 130 \text{ kPa s m}^2 \text{ kg}^{-1}$  at 1 mm to approximately  $\pm 160 \text{ kPa s m}^2 \text{ kg}^{-1}$  at 5mm for product processed with controlled nucleation (Fig. 9B; calculated considering  $\pm 3$  times the SD limited to positive values, that includes approximately 99 % of the vials).

#### **4.3. Impact of the product resistance variability on the product temperature distribution**

In order to optimize the primary drying step while maintaining an acceptable product quality, the product temperature has to be maintained close to a critical value but always to remain below it (e.g. glass transition temperature for amorphous product). The mass transfer heterogeneity resulting from differences in the product resistance among vials causes variability in the product temperature within the same batch or in different batches. Considering a constant value of the vial heat transfer coefficient (reported in Table 2), the distributions of the product temperature caused by the product resistance variability in a large batch of vials were calculated as reported in §3.3. Product resistance distributions previously determined for a 5 % w/w sucrose solution processed were considered with and without controlled nucleation and at -25 °C and 10 Pa during sublimation, as shown in Fig. 9. Product temperature distributions were determined for two different dried layer thicknesses, i.e. 1 mm and 5 mm and are reported in Fig. 10. As expected, the value of product temperature increased at higher dried layer thickness, because of the higher product resistance value.

Variability of the product temperature resulting from the product resistance distribution alone was estimated as  $\pm 3$  times the SD and was found to be approximately  $\pm 4.1$  °C at 1 mm and  $\pm 4.7$  °C at 5 mm for spontaneous nucleation (Fig. 10A). If the controlled nucleation is used, the variability is  $\pm 4.1$  °C at 1 mm and  $\pm 4.2$  °C at 5 mm (Fig. 10B). This variability of the product temperature is significantly greater than the one estimated by Scutellà et al. [16] due to the inter-vial  $K_V$  variability in central vials, which was reported to be approximately  $\pm 1$  °C. Only few other studies estimated the product temperature variability from the mass transfer difference in the vial batch [13, 41]. Pisano et al. [13] and Bosca et al. [41] reported product temperature variability resulting from the combined effect of the heat and mass transfer variability close to  $\pm 3$  °C for product processed with spontaneous nucleation in a pilot scale freeze-dryer. This value is lower than the product temperature variability estimated in this study by using the batch/global method for manufacturing scale, i.e. approximately  $\pm 4.4$  °C, but it is similar to the value estimated by using the local/single vial method (gravimetric method) for pilot scale, i.e. approximately  $\pm 3.5$  °C. The variability of the product temperature at pilot scale can be significantly lower than the variability at manufacturing scale. An environment with high level of particles, as the non-GMP laboratory, can lead to a lower value and smaller distribution of the nucleation temperature and thus in a lower mass transfer variability achieved in the product respect environment with low level of particles [25].

Based on this analysis, the risk of failure of the process can be estimated. As example, considering the glass transition temperature of the sucrose ( $-32$  °C) and a cycle performed at  $-25$  °C and 10 Pa, approximately 1 % of the vials processed with spontaneous nucleation will present a greater temperature than the critical value at a dried layer thickness of 5 mm (Fig. 10A). In order to guarantee that all the vials will present a temperature lower than the critical one, the shelf temperature should be reduced to approximately  $-28$  °C (for a constant pressure of 10 Pa). Conversely, no vials processed with controlled nucleation will present a temperature greater than the critical value.

## 5. Conclusions

The product resistance to mass transfer highly affects the value of the product temperature during the freeze-drying cycles. Thus, the value and variability of this parameter needs to be precisely evaluated for a reliable prediction of the product temperature. In this work, an approach was proposed to estimate the variability of the product resistance in batch of vials at

manufacturing and pilot scale by using two experimental strategies, a global/batch method (the pressure rise test) and a local/single vial one (the gravimetric method). The impact of the presence of stoppers in the vial necks and of the freezing protocol on the mass transfer were also considered. The presence of stoppers on the vials was not found to significantly modify the mass flow rate during sublimation. In contrast, the use of controlled nucleation during the freezing step of the freeze-drying cycle increased the mass flow rate with respect to cycles carried out with spontaneous nucleation and it decreased the mass flow rate variability.

The product resistance variability in a manufacturing vial batch, expressed in terms of standard deviation of the parameters  $R_{p_0}$  and  $R_{p_1}$ , was estimated based on pressure rise test data from 5 pilot vial batches. The standard deviations of  $R_{p_0}$  and  $R_{p_1}$  with controlled nucleation were observed to be lower than the variability of the resistance in batch processed with spontaneous nucleation. Furthermore, the variability of the product resistance between vials within a pilot batch was estimated with data from the gravimetric method and was found to be lower than the one obtained from the PRT, representative of a manufacturing batch of vials. The product resistance distributions determined from the PRT was used to calculate the product temperature distributions, which resulted in a variability of approximately  $\pm 4.4$  °C.

Finally, as an example of practical application, the presented approach was used for evaluating the risk of failure of the process resulting from the mass transfer variability only, expressed as a potential percentage of vials showing a product temperature higher than the critical value. The proposed approach will be used in the future to investigate the variability of the product resistance among vials presenting low filling volume (e.g. 0.4-0.5 ml) and processed with spontaneous nucleation in environmental conditions similar to those of Good Manufacturing Practice (GMP) in a production scale (i.e. less presence of particle in the air).

## Nomenclature

$A$	Cross sectional area ( $m^2$ )
$df$	Degrees of freedom
$\Delta H$	Latent heat of sublimation ( $J kg^{-1}$ )
$K_V$	Vial heat transfer coefficient ( $W m^{-2}K^{-1}$ )
$l$	Layer thickness ( $m$ )
$\Delta m(t_{sub})$	Sublimed mass at time $t_{sub}$ ( $kg$ )
$\dot{m}$	Mass flow rate ( $\frac{kg}{s}$ )
$M_W$	Molecular weight of water ( $kg kmol^{-1}$ )
$N_V$	Number of vials
$P$	Pressure ( $Pa$ )
$\dot{Q}$	Heat flow rate ( $W$ )
$R_g$	Ideal gas constant ( $J K^{-1}kmol^{-1}$ )
$R_p$	Product resistance ( $Pa m^2 s kg^{-1}$ )
$SD$	Standard deviation
$SE$	Standard error ( $SE = \frac{SD}{\sqrt{df}}$ , see (9))
$t_{sub}$	Sublimation time ( $s$ )
$T$	Temperature ( $K$ )
$V$	Volume ( $m^3$ )

## Greek

$\lambda$	Thermal conductivity ( $W m^{-1} K^{-1}$ )
$\rho$	Density of ice ( $kg m^{-3}$ )

## Subscripts

0,1	Index of parameters in Eq. (6)
$B$	Bottom
$C$	Chamber
$d$	Dried
$f$	Frozen
$i$	Interface
$S$	Shelf
$v$	Vapour

V Vial

## References

- [1] L.J.J. Hansen, R. Daoussi, C. Vervaet, J.P. Remon, T.R.M. De Beer, Freeze-drying of live virus vaccines: A review, *Vaccine* 33 (2015) 5507-5519.
- [2] G.D.J. Adams, Freeze-Drying of Biological Materials, *Drying Technol.* 9 (1991) 891-925.
- [3] F. Fonseca, S. Cenard, S. Passot, Freeze-Drying of Lactic Acid Bacteria, in: W.F. Wolkers, H. Oldenhof (Eds.), *Cryopreservation and Freeze-Drying Protocols*, Springer New York, New York, NY, 2015, pp. 477-488.
- [4] L.L.R. Johnson, Freeze-drying protein formulations above their collapse temperatures: Possible issues and concerns, *Am. Pharm. Rev.* 14 (2011) 50-54.
- [5] S.M. Patel, S.L. Nail, M.J. Pikal, R. Geidobler, G. Winter, A. Hawe, J. Davagnino, S. Rambhatla Gupta, Lyophilized Drug Product Cake Appearance: What Is Acceptable?, *J. Pharm. Sci.* 106 (2017) 1706-1721.
- [6] M.J. Pikal, S. Shah, The collapse temperature in freeze drying: Dependence on measurement methodology and rate of water removal from the glassy phase, *Int. J. Pharm.* 62 (1990) 165-186.
- [7] M.J. Pikal, W.J. Mascarenhas, H.U. Akay, S. Cardon, C. Bhugra, F. Jameel, S. Rambhatla, The Nonsteady State Modeling of Freeze Drying: In-Process Product Temperature and Moisture Content Mapping and Pharmaceutical Product Quality Applications, *Pharm. Dev. Technol.* 10 (2005) 17-32.
- [8] I.C. Trelea, S. Passot, F. Fonseca, M. Marin, An Interactive Tool for the Optimization of Freeze-Drying Cycles Based on Quality Criteria, *Drying Technol.* 25 (2007) 741-751.
- [9] S.A. Velardi, A.A. Barresi, Development of simplified models for the freeze-drying process and investigation of the optimal operating conditions, *Chem. Eng. Res. Des.* 86 (2008) 9-22.
- [10] A. Giordano, A.A. Barresi, D. Fissore, On the use of mathematical models to build the design space for the primary drying phase of a pharmaceutical lyophilization process, *J. Pharm. Sci.* 100 (2011) 311-324.
- [11] E. Lopez-Quiroga, L.T. Antelo, A.A. Alonso, Time-scale modeling and optimal control of freeze-drying, *J. Food Eng.* 111 (2012) 655-666.
- [12] M.J. Pikal, M.L. Roy, S. Shah, Mass and heat transfer in vial freeze-drying of pharmaceuticals: Role of the vial, *J. Pharm. Sci.* 73 (1984) 1224-1237.
- [13] R. Pisano, D. Fissore, A.A. Barresi, P. Brayard, P. Chouvenec, B. Woinet, Quality by design: optimization of a freeze-drying cycle via design space in case of heterogeneous

drying behavior and influence of the freezing protocol, *Pharm. Dev. Technol.* 18 (2013) 280-295.

[14] S. Hibler, C. Wagner, H. Gieseler, Vial freeze-drying, part 1: new insights into heat transfer characteristics of tubing and molded vials, *J. Pharm. Sci.* 101 (2012) 1189-1201.

[15] R. Pisano, A.A. Barresi, D. Fissore, Heat transfer in freeze-drying apparatus, in: M. dos Santos Bernardes (Ed.), *Developments in Heat Transfer*, INTECH, Rijeka, Croatia, 2011, pp. 91–114.

[16] B. Scutellà, S. Passot, E. Bourles, F. Fonseca, I.C. Trelea, How Vial Geometry Variability Influences Heat Transfer and Product Temperature During Freeze-Drying, *J. Pharm. Sci.* 106 (2017) 770-778.

[17] M.J. Pikal, S. Shah, D. Senior, J.E. Lang, Physical Chemistry of Freeze-drying: Measurement of Sublimation Rates for Frozen Aqueous Solutions by a Microbalance Technique, *J. Pharm. Sci.* 72 (1983) 635-650.

[18] J. Xiang, J.M. Hey, V. Liedtke, D.Q. Wang, Investigation of freeze-drying sublimation rates using a freeze-drying microbalance technique, *Int. J. Pharm.* 279 (2004) 95-105.

[19] D. Fissore, R. Pisano, A.A. Barresi, On the Methods Based on the Pressure Rise Test for Monitoring a Freeze-Drying Process, *Drying Technol.* 29 (2010) 73-90.

[20] I. Oddone, R. Pisano, R. Bullich, P. Stewart, Vacuum-Induced Nucleation as a Method for Freeze-Drying Cycle Optimization, *Ind. Eng. Chem. Res.* 53 (2014) 18236-18244.

[21] X.C. Tang, S.L. Nail, M.J. Pikal, Evaluation of manometric temperature measurement (MTM), a process analytical technology tool in freeze drying, part III: Heat and mass transfer measurement, *AAPS PharmSciTech* 7 (2014) E105-E111.

[22] W.Y. Kuu, K.R. O'Bryan, L.M. Hardwick, T.W. Paul, Product mass transfer resistance directly determined during freeze-drying cycle runs using tunable diode laser absorption spectroscopy (TDLAS) and pore diffusion model, *Pharm. Dev. Technol.* 16 (2011) 343-357.

[23] W.Y. Kuu, L.M. Hardwick, M.J. Akers, Rapid determination of dry layer mass transfer resistance for various pharmaceutical formulations during primary drying using product temperature profiles, *Int. J. Pharm.* 313 (2006) 99-113.

[24] S. Bosca, A.A. Barresi, D. Fissore, Use of a soft sensor for the fast estimation of dried cake resistance during a freeze-drying cycle, *Int. J. Pharm.* 451 (2013) 23-33.

[25] J.A. Searles, J.F. Carpenter, T.W. Randolph, The ice nucleation temperature determines the primary drying rate of lyophilization for samples frozen on a temperature-controlled shelf, *J. Pharm. Sci.* 90 (2001) 860-871.

- [26] A.K. Konstantinidis, W. Kuu, L. Otten, S.L. Nail, R.R. Sever, Controlled nucleation in freeze-drying: effects on pore size in the dried product layer, mass transfer resistance, and primary drying rate, *J. Pharm. Sci.* 100 (2011) 3453-3470.
- [27] J.A. Searles, Freezing and Annealing Phenomena in Lyophilization, in: L. Rey, J.C. May (Eds.), *Freeze-Drying/Lyophilization of Pharmaceutical and Biological Products*, CRC Press, London, UK, 2010, pp. 52–81.
- [28] S. Passot, I.C. Trelea, M. Marin, M. Galan, G.J. Morris, F. Fonseca, Effect of controlled ice nucleation on primary drying stage and protein recovery in vials cooled in a modified freeze-dryer, *J. Biomech. Eng.* 131 (2009) 074511.
- [29] I. Oddone, P.J. Van Bockstal, T. De Beer, R. Pisano, Impact of vacuum-induced surface freezing on inter- and intra-vial heterogeneity, *Eur. J. Pharm. Biopharm.* 103 (2016) 167-178.
- [30] M.J. Pikal, Heat and Mass Transfer in Low Pressure Gases: Applications to Freeze Drying, in: G.L. Amidon, P.I. Lee, E.M. Topp (Eds.), *Transport Processes in Pharmaceutical Systems*, Marcel Dekker, New York, 2000.
- [31] D.E. Overcashier, T.W. Patapoff, C.C. Hsu, Lyophilization of protein formulations in vials: investigation of the relationship between resistance to vapor flow during primary drying and small-scale product collapse, *J. Pharm. Sci.* 88 (1999) 688-695.
- [32] D. Fissore, R. Pisano, Computer-Aided Framework for the Design of Freeze-Drying Cycles: Optimization of the Operating Conditions of the Primary Drying Stage, *Processes* 3 (2015) 406-421.
- [33] T. Kodama, H. Sawada, H. Hosomi, M. Takeuchi, N. Wakiyama, E. Yonemochi, K. Terada, Determination for dry layer resistance of sucrose under various primary drying conditions using a novel simulation program for designing pharmaceutical lyophilization cycle, *Int. J. Pharm.* 452 (2013) 180-187.
- [34] A. Saltelli, M. Ratto, T. Andres, F. Campolongo, J. Cariboni, D. Gatelli, M. Saisana, S. Tarantola, *Global Sensitivity Analysis: The Primer*, Wiley, Chichester, UK, 2008.
- [35] G.D. Smith, *Numerical solution of partial differential equations: finite difference methods*, Clarendon Press, Oxford, New York, 1985.
- [36] P. Sheehan, A.I. Liapis, Modeling of the primary and secondary drying stages of the freeze drying of pharmaceutical products in vials: numerical results obtained from the solution of a dynamic and spatially multi-dimensional lyophilization model for different operational policies, *Biotechnol. Bioeng.* 60 (1998) 712-728.

- [37] K.H. Gan, R. Bruttini, O.K. Crosser, A.I. Liapis, Freeze-drying of pharmaceuticals in vials on trays: effects of drying chamber wall temperature and tray side on lyophilization performance, *Int. J. Heat Mass Transfer* 48 (2005) 1675-1687.
- [38] A. Arsiccio, R. Pisano, Application of the Quality by Design Approach to the Freezing Step of Freeze-Drying: Building the Design Space, *J. Pharm. Sci.* In press (2018).
- [39] S. Mortier, P.J. Van Bockstal, J. Corver, I. Nopens, K.V. Gernaey, T. De Beer, Uncertainty analysis as essential step in the establishment of the dynamic Design Space of primary drying during freeze-drying, *Eur. J. Pharm. Biopharm.* 103 (2016) 71-83.
- [40] S. Rambhatla, R. Ramot, C. Bhugra, M.J. Pikal, Heat and mass transfer scale-up issues during freeze drying: II. Control and characterization of the degree of supercooling, *AAPS PharmSciTech* 5 (2004) 54-62.
- [41] S. Bosca, A.A. Barresi, D. Fissore, M. Deamichela, Risk-Based Design of a Freeze-Drying Cycle for Pharmaceuticals, in: *EMChIE 2015 Conference Proceedings*, Arts Gràfiques Rabassa, S.A., Tarragona, Spain, 2015, pp. 265–270.

## **ACKNOWLEDGMENTS**

The authors would like to thank Yves Mayeresse and Moritz von Stosch (GSK) for reviewing this work.

## **CONFLICT OF INTEREST**

Erwan Bourlès and Bernadette Scutellà are employees of the GSK group of companies. Stephanie Passot, Fernanda Fonseca, and Ioan Cristian Trelea report no financial conflicts of interest.

## **FUNDING**

This work was funded by GlaxoSmithKline Biologicals S.A., under a Cooperative Research and Development Agreement with INRA (Institut National de la Recherche Agronomique) via the intermediary of the UMR (Unité Mixte de Recherche) GMPA (Génie et Microbiologie des Procédés Alimentaires) at the INRA Versailles-Grignon research centre.

## **AUTHORS CONTRIBUTIONS**

Bernadette Scutellà acquired the data. Bernadette Scutellà, Stephanie Passot, Erwan Bourlès, Fernanda Fonseca and Ioan Cristian Trelea analyzed and interpreted the experimental results. All authors were involved in drafting the manuscript or revising it critically for important intellectual content. All authors had full access to the data and approved the manuscript before it was submitted by the corresponding author.

## Tables

**Table 1:** Description of the sublimation experiments performed in this study.

<i>Description</i>	<i>PRT method</i>	<i>Gravimetric+PRT method</i>
Vials filled with sucrose solution and processed without stoppers (S5)	S5-1	S5-4
	S5-2	S5-5
	S5-3	
Vials filled with sucrose solution and processed with partially inserted stoppers (S5s)	S5s-1	
	S5s-2	
Vials filled with sucrose solution + 0.1% of Snomax to control the nucleation and processed without stoppers (S5cn)	S5cn-1	S5cn-4
	S5cn-2	S5cn-5
	S5cn-3	

**Table 2:** Vial and freeze-dryer dimensions, physical properties and parameters used in this study

<i>Symbol</i>	<i>Significance</i>	<i>Value <math>\pm</math> SD</i>	<i>Units</i>
$A_{BV}$	Outer bottom area of the vial	$2.07 \cdot 10^{-4}$	$m^2$
$A_i$	Inner bottom area of the vial	$1.78 \cdot 10^{-4}$	$m^2$
$\Delta H$	Latent heat of sublimation of ice	$2.8 \cdot 10^6$	$J \cdot kg^{-1}$
$K_V$	Vial heat transfer coefficient <sup>a</sup>	$13.30 \pm 0.885$	$W \cdot m^{-2} \cdot K^{-1}$
$\lambda_f$	Ice thermal conductivity	2.23	$W \cdot m^{-1} \cdot K^{-1}$
$\rho$	Density of ice	917	$kg \cdot m^{-3}$
$R_g$	Ideal gas constant	$8.314 \cdot 10^3$	$J \cdot K^{-1} \cdot kmol^{-1}$
$T_C$	Temperature of the drying chamber	242	$K$
$M_W$	Water molecular weight	18	$kg \cdot kmol^{-1}$
$V_C$	Volume of the drying chamber	0.12	$m^3$

SD, standard deviation.

<sup>a</sup> Evaluated from Scutellà et al. [16]

**Table 3:** Mean  $\pm$  standard deviation (SD) for the sets of coefficients  $Rp_0$  and  $Rp_1$  (Eq. (6)) from data of experiments S5 and S5cn.

<i>Set of parameters</i>	<i>Pressure rise test</i>				<i>Gravimetric method</i>	
	$Rp_0$		$Rp_1$		$Rp_1$	
	[kPa s m <sup>2</sup> kg <sup>-1</sup> ]		[kPa s m kg <sup>-1</sup> ]		[kPa s m kg <sup>-1</sup> ]	
	<i>Mean</i>	<i>SD</i>	<i>Mean</i>	<i>SD</i>	<i>Mean</i>	<i>SD</i>
	$\widetilde{Rp}_0$		$\widetilde{Rp}_1$		$\widetilde{Rp}_1$	
S5	59	75	1.8 10 <sup>4</sup>	2.0 10 <sup>4</sup>	1.8 10 <sup>4</sup>	0.3 10 <sup>4</sup>
S5cn	47	48	0.9 10 <sup>4</sup>	1.2 10 <sup>4</sup>	0.9 10 <sup>4</sup>	0.2 10 <sup>4</sup>

see Table 1 for the experimental conditions of experiments S5 and S5cn.

**Table 4:** Comparison of the product resistance value  $R_p$  obtained in this study with other values reported in literature for a 5 % sucrose solution and a dried layer thickness  $l_d$  of 5 mm.

<i>Reference</i>	<i>Primary drying conditions</i>	<i>Nucleation during freezing step</i>	$R_p$ at $l_d = 5$ mm [kPa m <sup>2</sup> s kg <sup>-1</sup> ]
This work	Performed at a shelf temperature of -25 °C and a chamber pressure of 10 Pa	Spontaneous	149
		Controlled <sup>a</sup> at -4 °C	92
Konstantinidis et al. [26]	Shelf temperature ramping from -35 °C to -10 °C at 0.02 °C min <sup>-1</sup> , and chamber pressure of 13 Pa	Spontaneous	125
		Controlled <sup>b</sup> at -3 °C	91
Bosca et al. [24]	Performed at a shelf temperature of -20 °C and a chamber pressure of 10 Pa	Spontaneous	~ 145 <sup>d</sup>
Rambhatla et al. [40]	Performed at a shelf temperature of -25 °C and a chamber pressure of 13 Pa	Controlled <sup>c</sup> at -1 °C	67 <sup>d</sup>
		Controlled <sup>c</sup> at -6 °C	77 <sup>d</sup>
		Controlled <sup>c</sup> at -11 °C	96 <sup>d</sup>
Fissore et al. [32]	Performed at a shelf temperature of -30 °C and a chamber pressure of 5 Pa	Spontaneous	~ 100 <sup>d</sup>

<sup>a</sup> Nucleation agent Snomax (§2.2)

<sup>b</sup> Nucleation induced by creating the vacuum in the drying chamber during the freezing step

<sup>c</sup> Improved ice fog technique

<sup>d</sup> Graphically interpolated from the  $R_p$  vs  $l_d$  data reported in the cited works

## Figures

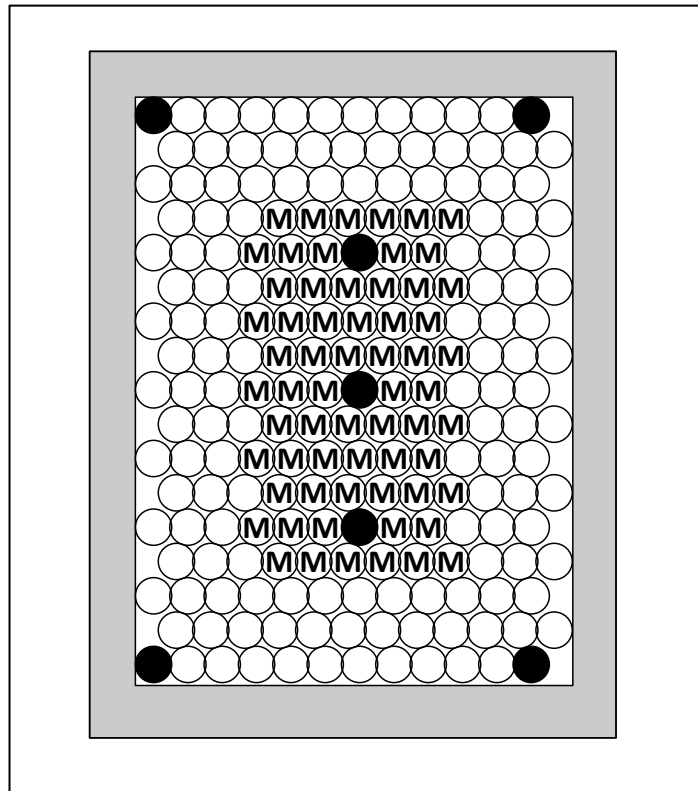


**Fig. 1:** Arrangement of the vials on the shelf. Symbols: black circle, vials in which the thermocouples are located; Letter 'M', gravimetrically-analyzed vials. All vials were filled with 1.8 mL of the selected product.

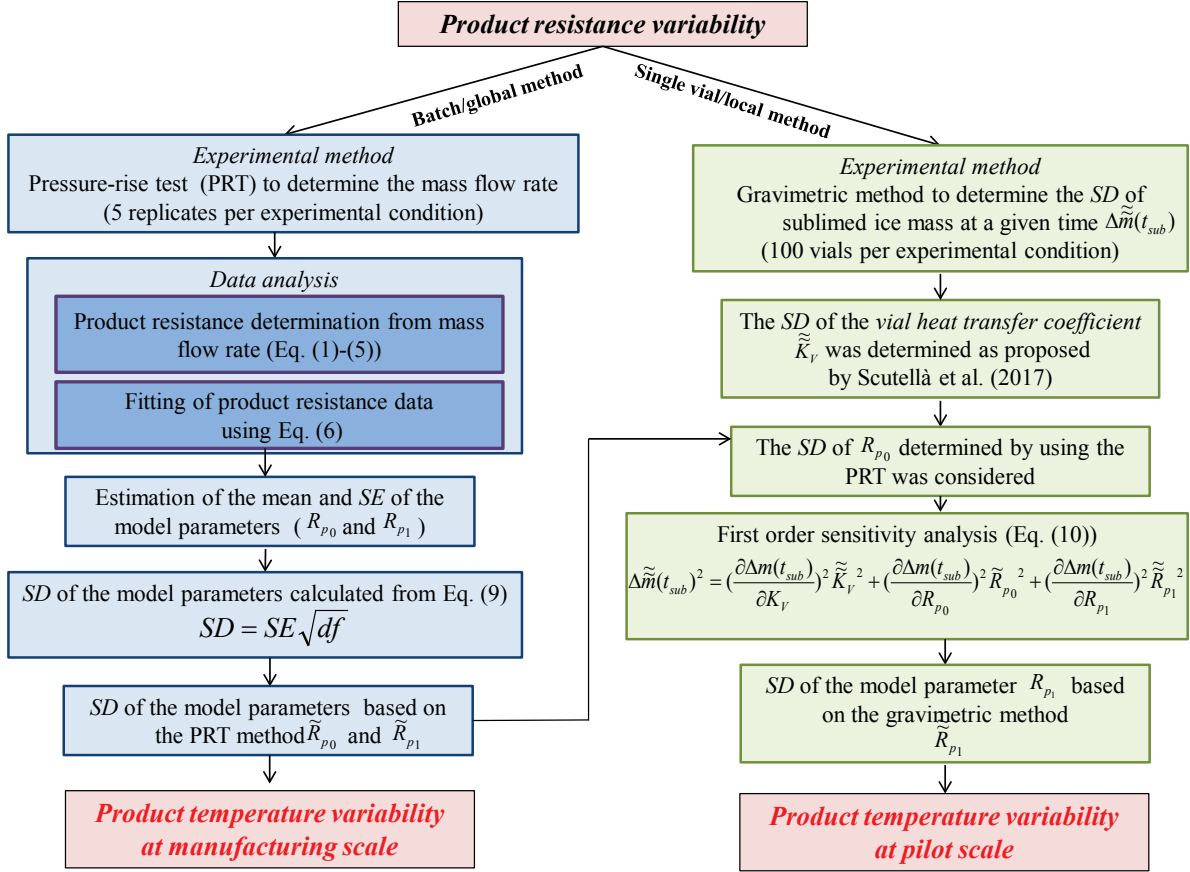


**Fig. 2:** Flow chart used to determine the product resistance variability using the pressure rise test (PRT) and the gravimetric methods. SD: standard deviation; SE: standard error.

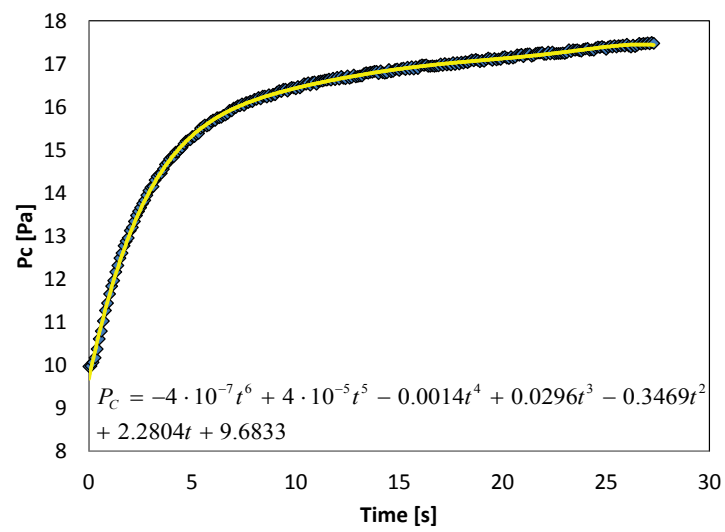


**Fig. 3:** Example of the increase of the chamber pressure in time during a pressure rise test (PRT) performed during the freeze-drying cycles S5-1 (spontaneous nucleation).

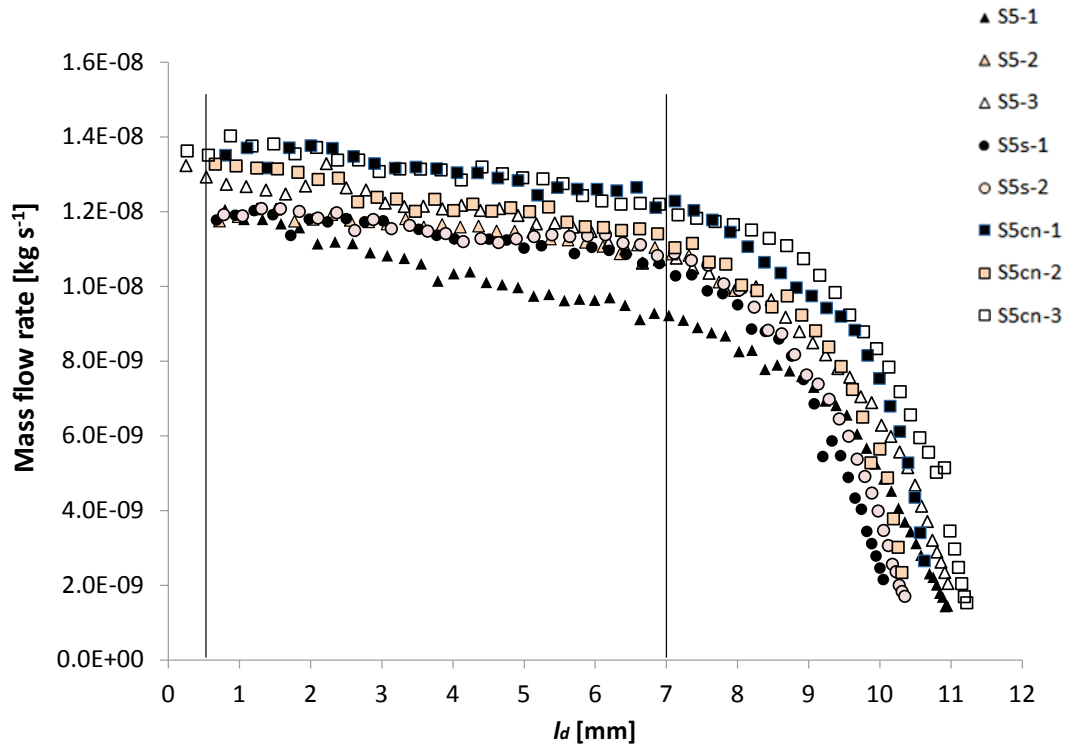


**Fig. 4:** Mass flow rates evolution as a function of the dried thickness in freeze-drying tests of 5 % sucrose solution processed in vials without stoppers and spontaneous nucleation (S5, triangles), with partially inserted stoppers and spontaneous nucleation (S5s, circles) and without stoppers and controlled nucleation (S5cn, squares). The mass flow rates were determined by the PRT method from Eq. (8). Vertical solid lines represent the mass flow rates data range considered in the analysis.

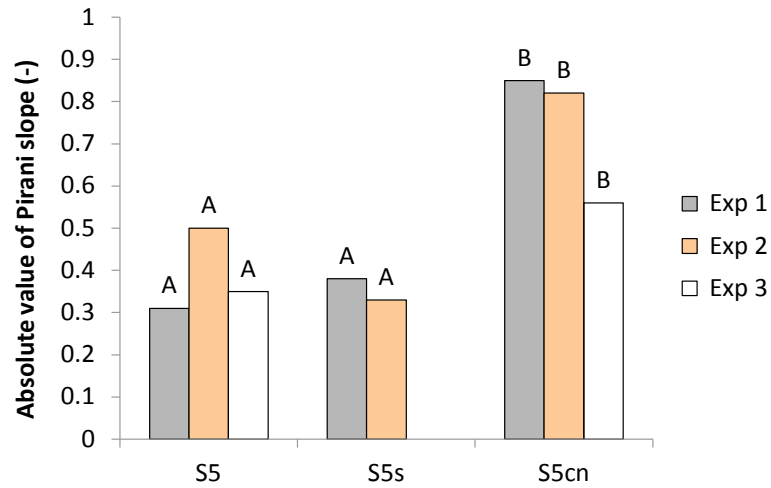


**Fig. 5:** Absolute value of Pirani slope at the end of sublimation obtained from freeze-drying cycles performed with product processed in vials without stoppers and spontaneous nucleation (S5), with partially inserted stoppers and spontaneous nucleation (S5s) and without stoppers and with controlled nucleation (S5cn). Experiments marked with the letter A in the legend show a significant difference at 0.05 level than experiments marked with the letter B (ANOVA test).

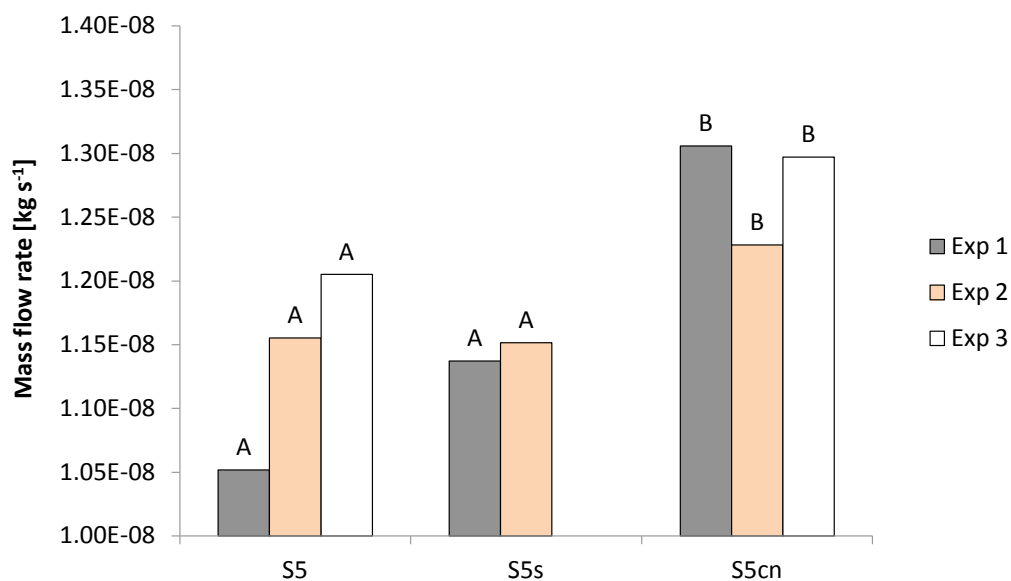


**Fig. 6:** Average values of the mass flow rates within a range of dried layer thickness between 0.5 mm and 7 mm in case of product processed in vials without stoppers and spontaneous nucleation (S5), with partially inserted stoppers and spontaneous nucleation (S5s) and without stoppers and with controlled nucleation (S5cn). Experiments marked with the letter A in the legend show a significant difference at 0.05 level than experiments marked with the letter B (ANOVA test).

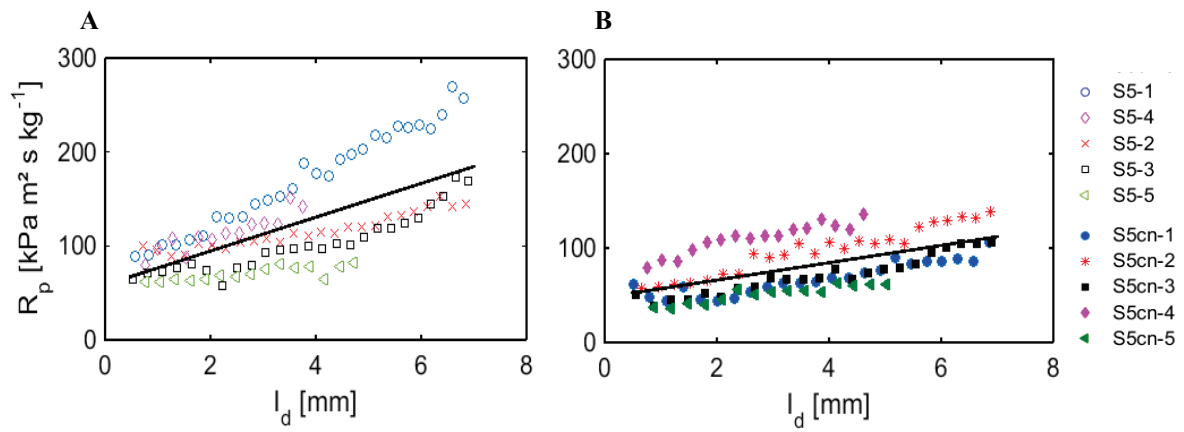


**Fig. 7:** Evolution of the product resistance with the dried layer thickness calculated from PRT data obtained in tests performed without stoppers and spontaneous nucleation (S5) (Fig. 6A) and PRT data obtained in tests performed without stoppers and with controlled nucleation (S5cn) (Fig. 6B). Symbols: experimental data; Solid line: fitting of the experimental data with Eq. (6).

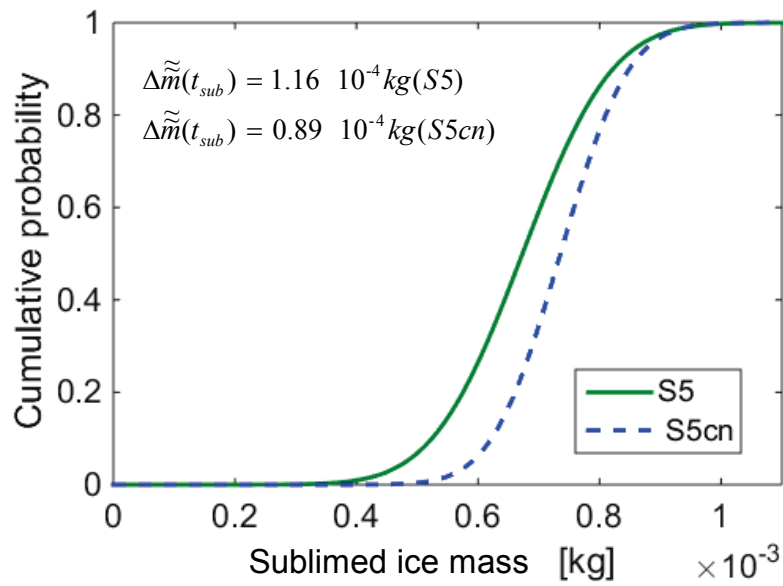


**Fig. 8:** Cumulative probability of the water mass loss determined from data obtained by using the gravimetric method in cycles performed with spontaneous nucleation (S5, dotted line) and controlled nucleation (S5cn, dashed line). The standard deviation of the mass loss for the two sets of data is reported on the figure.

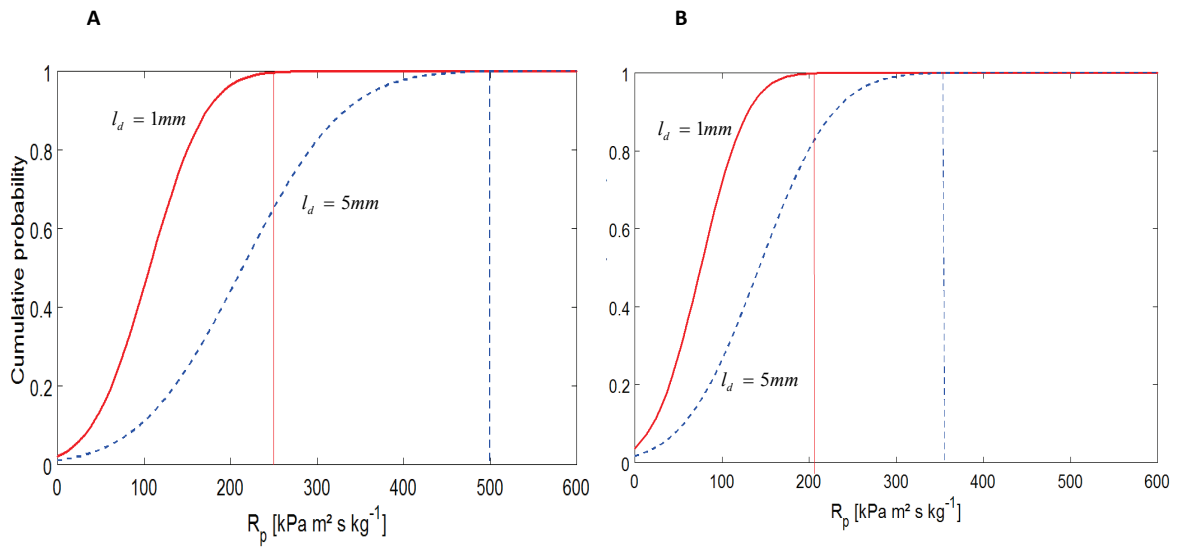


**Fig. 9:** Cumulative probability distributions of the product resistance obtained from the set of parameters obtained with spontaneous nucleation (S5) (Fig. 8A) and with controlled nucleation (S5cn) (Fig. 8B). Solid and dotted bold lines represent respectively the product resistance distribution at 1 mm and 5 mm. Vertical lines include approximately 99 % of values of the product resistance.

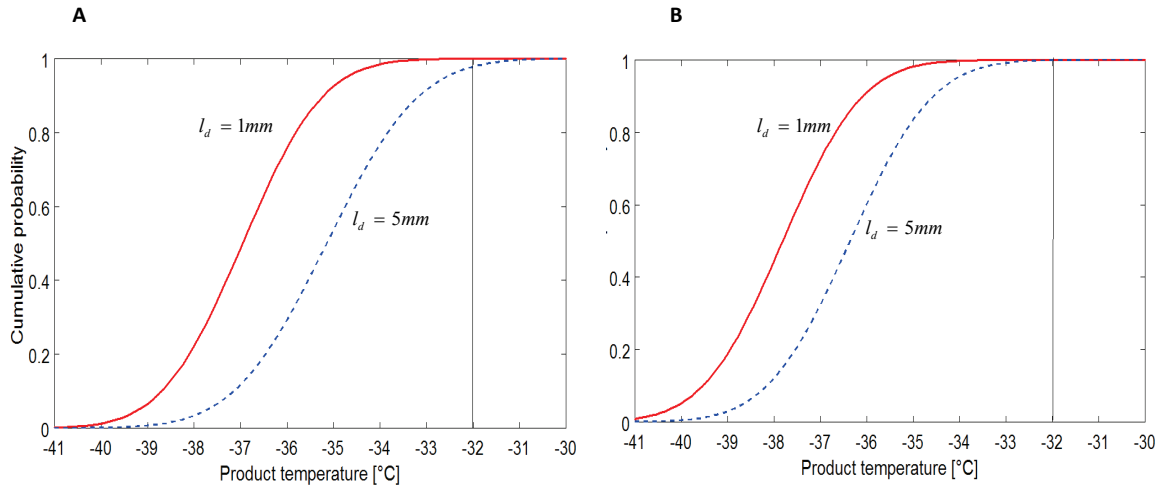


**Fig. 10:** Cumulative probability distributions of the product temperature obtained for freeze-drying cycles carried out with spontaneous nucleation (S5) (Fig. 9A) and without controlled nucleation (S5cn) (Fig. 9B). Solid and dotted lines represent the product resistance distribution at 1 mm and 5 mm respectively. Vertical lines represent the critical product temperature ( $-32^{\circ}C$  for sucrose).